Fluid Dynamics & Materials Processing FDMP, vol.15, no.3, pp.271-284, 2019

Analysis of the Impact of the Space Guide Vane Wrap Angle on the Performance of a Submersible Well Pump

Xiaorui Cheng[1, 2, *], Hongxing Chen[1] and Xiaoquan Wang[1]

Abstract: In order to study the influence of the wrap angle relating to the space guide vane of a submersible well pump (250*QJ*125) on the flow field and pump performance, seven possible configurations have been considered (obtained by changing the blade wrap angle while keeping unchanged all the other parameters). Such configurations have been numerically simulated in the framework of a computational model based on the Reynolds time-averaged N-S equations, the RNG k-ε turbulence approach and the SIMPLE algorithm. The impact exerted by different wrap angles of the guide vane on the performance of the pump, the internal losses of the guide vane and the flow field distribution in the bladeless area at the guide vane outlet has been assessed via cross-comparison of all these cases. The results show that the wrap angle has a significant influence: the wrap angle with the highest head is different from that with the highest efficiency, and changes in this angle have a more significant effect on the head than efficiency. A moderate raise of the wrap angle can improve the properties of the flow, reduce turbulence losses and enhance the energy conversion rate inside the guide vane. Different wrap angles can also lead to different fluid circulation modes in the bladeless area from guide vane outlet to impeller inlet, while they have a weak influence on the absolute value of the velocity of the fluid entering the impeller.

Keywords: Submersible well pump, space guide vane, wrap angle, internal flow.

1 Introduction

Submersible well pumps, the main equipment for working in wells, have been widely used in various fields of industry and agriculture. The main function of guide vane is to collect the liquid flowing out of the impeller and transport it to the impeller entrance of next stage or pump exit. At the same time, the direction of flow is adjusted to eliminate the velocity circulation of flow, so as to ensure the relatively stable flow of fluid in impeller [Yang, Li, Gao et al. (2008)]. As a core component of pump, its shape and hydraulic parameters have a huge impact on the performance of pump [Guan (2011)]. Therefore, the optimization design of the space guide vane is important for improving the overall performance of the pump.

Numerous relevant scholars have successively carried out a series of in-depth studies about

[1] Lanzhou University of Technology, College of Energy and Power Engineering, Lanzhou, 730050, China.

[2] Key Laboratory of Fluid machinery and Systems of Gansu Province, Lanzhou, 730050, China.

[*] Corresponding Author: Xiaorui Cheng. Email: cxr168861@sina.com.

space guide vane as follows: the optimal design methods of structure [Cheng, Lv, Zhang et al. (2018); Zhou, Bai, Yang et al. (2016); Cresswell, Ingram and Dominy (2015)], the analysis of internal flow field [Yang and Wang (2018); Han, Chen, Liu et al. (2018); Koirala, Neopane, Shrestha et al. (2017); Chitrakar, Thapa, Dahlhaug et al. (2017)] and the improvement to the properties of flow [Zhou, Hu and Zhang (2015); Zhou, Shi, Lu et al. (2011); Zhou, Shi and Lu (2011)] confirmed that the three-dimensional curved guide vane had fewer hydraulic losses than the cylindrical guide vane in the deep-well centrifugal pump through numerical simulation method. Zhang et al. [Zhang, Guo, Yang et al. (2015)] studied the relationship between the wrap angles of guide vane and the efficiency of centrifugal pumps. Cong et al. [Cong, Zhou, Han et al. (2015)] performed the orthogonal test with four parameters of space guide vane, and concluded that the attack angle and wrap angle produced great effect on the head and efficiency of the pump. Liang et al. [Liang, Lu, Xu et al. (2012)] verified the existence of the optimal velocity circulation which could minimize the hydraulic losses of guide vane passage by numerical calculation and experiment. Multitudinous scholars have paid great attention to the optimization of key geometric parameters of space guide vane, but the research on the effect of guide vane on the energy conversion rate, internal flow characteristics and fluid circulation modes of impeller inlet is not enough.

The space guide vane of submersible well pump was taken as the research object in this paper. The relationship between the space guide vane with different wrap angles and the pump performance is studied by means of numerical simulation, so as to provide a theoretical foundation for mastering the internal flow properties of the space guide vane and improving the hydraulic design method.

2 Research model and method

2.1 Computational model

The basic hydraulic design parameters of 250*QJ*125 type submersible well pump are as follows: rated flow Q=125 m^3/h, single-stage head H=16 m, rated rotating speed n=2875 r/min, stage number=5, rated shaft power P_d=34.94 kW. The main structure parameters of impeller and guide vane are shown in Tab. 1. And the whole computational domain model and pump model are shown in Fig. 1.

Table 1: Main structure parameters of the impeller and guide vane

Component	Parameters	Value	Component	Parameters	Value
Impeller	Inlet diameter D_1 (mm)	98	Guide vane	Axial length L_1(mm)	101
	Outlet diameter D_2 (mm)	145		Blade number Z_2	8
	Blade number Z_1	7		Inlet angle of blade α_3 (°)	26
	Outlet angle of blade β_2(°)	30		Outlet angle of blade α_4(°)	90
	Wrap angle of blade Φ_1(°)	110		Wrap angle of blade Φ_2(°)	90

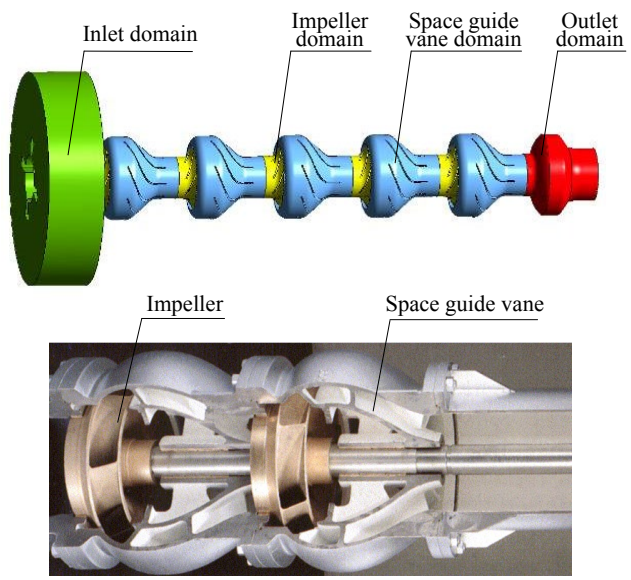

Figure 1: Fluid domain 3D model and structure diagram of the submersible well pump

2.2 Design scheme of space guide vane

The calculation model was the basic for the numerical calculation, and its integrity significantly influenced the numerical results. Hence, based on conformal mapping method, the meridional shape of space guide vane is drawn to ensure that guide vane can receive the liquid flowing from the impeller and smoothly connect the next impeller or pump exit. In order to analyse the effect of the wrap angle of the space guide vane on the performance of submersible well pump while keeping unchanged all the other parameters, seven possible configurations have been considered in this study and three-dimensional models of space guide vane with wrap angle of 60°, 70°, 80°, 90°, 100°, 110° and 120° are built respectively.

3 Numerical calculation

3.1 Analyzing grid independence

The whole computational domain was split in ICEM software based on unstructured tetrahedrons. Since the number of grids will directly affect the convergence and accuracy of calculation results, the independence of different grid numbers in the whole basin was verified. Theoretically, the calculating errors will decrease gradually with an increase in grid number, but too many grids will increase the computational period. Six different grid numbers were considered to calculate and analyse, the calculation results of grid sensitivity analysis for this model is shown in Tab. 2. The result with 1.809×10^7 or more elements had no significant difference of less than 0.1%, indicating that the simulation results are tending towards stable when the grid number is larger than 18 million. Considering the computer's calculation capability, 18 million elements scheme is selected to carry out the following study. The grids of impeller and guide vane are meshed as shown in Fig. 2.

Table 2: Grid independence test of submersible well pump

Grid density	5.415×10^6	9.614×10^6	1.482×10^7	1.809×10^7	2.062×10^7	2.573×10^7
Head (m)	99.27	100.47	101.32	101.94	101.96	101.93

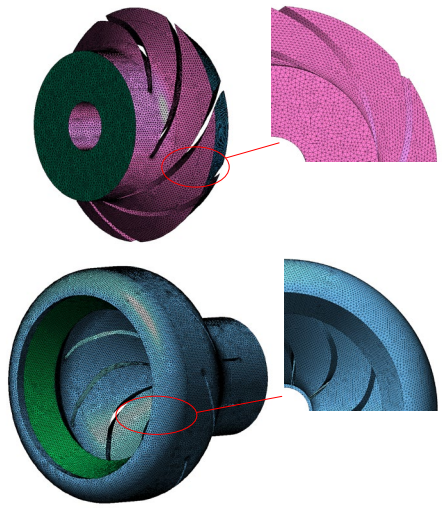

Figure 2: Computational grids of impeller and guide vane of submersible well pump

3.2 Boundary conditions

The whole flow condition was set as three-dimensional incompressible steady flow. The boundary conditions were assumed to be velocity at inlet and ouflow at the outlet. All walls of the flow domain were used non-slip boundary condition. The diffusion term is discretized by the second-order central difference scheme. Considering the convergence of the data, the convection term is discretized by the first-order upwind scheme. The pressure-velocity coupling was calculated by means of the SIMPLE algorithm. Residual convergence criterion was set to 10^{-4}. The continuous equation and momentum equation in the relative coordinate system were established. The steady governing equations are shown in the formula (1) and formula (2).

Continuity equation:

$$\frac{\partial u}{\partial x}+\frac{\partial v}{\partial y}+\frac{\partial w}{\partial z}=0 \tag{1}$$

where, u, v and w are the velocity components in three directions x, y and z respectively.

Momentum equation：

$$\frac{\partial\left(\rho u_i u_j\right)}{\partial x_i}=\mu\frac{\partial^2 u_i}{\partial x_i \partial x_j}-\frac{\partial p}{\partial x_i}+\rho F_i \tag{2}$$

where, $\rho u_i u_j$ is Reynolds stress, Pa; ρ is density of fluid, kg/m^3; p is pressure, Pa; ρF_i is the mass force acting on the fluid element, N; μ is turbulent viscosity, N·s/m^2.

3.3 Turbulence model

In this study, numerical calculations were performed in ANSYS-fluent code, which provides several turbulence models. Among the turbulence models, k-ε and k-ω are the most suitable for the internal flow of the rotating machines. Hence, four models (standard k-ε model, RNG k-ε model, standard k-ω model and SST k-ω model) are adopted to carry out the numerical calculations. Comparing their results with the test value, (as shown in Tab. 3) it can be found that all of the numerical results of four turbulence models are higher than test value, among which the result of RNG k-ε model is closest to the test value. Therefore, RNG k-ε model is selected for the following numerical calculation. The k and ε equations of turbulence model are as follows:

k equation:

$$\frac{\partial(\rho k)}{\partial t}+\frac{\partial(\rho k u_{\mathrm{j}})}{\partial x_{\mathrm{j}}}=\frac{\partial}{\partial x_{\mathrm{j}}}\left[\alpha_{\mathrm{k}}\mu_{\mathrm{eff}}\frac{\partial k}{\partial x_{\mathrm{j}}}\right]+G_{\mathrm{k}}+\rho\varepsilon \tag{3}$$

ε equation:

$$\frac{\partial(\rho\varepsilon)}{\partial t}+\frac{\partial(\rho\varepsilon u_{\mathrm{i}})}{\partial x_{\mathrm{i}}}=\frac{\partial}{\partial x_{\mathrm{j}}}\left[\alpha_{\varepsilon}\mu_{\mathrm{eff}}\frac{\partial\varepsilon}{\partial x_{\mathrm{j}}}\right]+\frac{C_{1\varepsilon}\varepsilon}{k}G_{\mathrm{k}}-C_{2\varepsilon}\rho\frac{\varepsilon^{2}}{k} \tag{4}$$

$$\mu_{\mathrm{eff}}=\mu+\mu_{\mathrm{t}} \tag{5}$$

$$\mu_{\mathrm{t}}=\rho C_{\mu}\frac{k^{2}}{\varepsilon} \tag{6}$$

where C_{μ}, α_{k}, α_{ε} are the empirical constants equal 0.0845, 1.39 and 1.39, respectively; G_{k} is generation term for turbulent kinetic energy; ε is turbulent dissipation rate; $C_{1\varepsilon}$, $C_{2\varepsilon}$ are the empirical constants equal 1.44 and 1.92, respectively [Liu, Wang, Liu et al. (2013)].

Table 3: Numerical and experimental results with different turbulent models

Turbulence model	Standard k-ε	RNG k-ε	Standard k-ω	SST k-ω	Test value
Efficiencyη (%)	86.97	86.05	88.21	87.91	85.01
Error (to test value)	2.33%	1.24%	3.78%	3.42%	
Head H (m)	101.99	101.94	103.13	102.84	100.91
Error (to test value)	1.1%	1.0%	2.21%	1.92%	

4 Test verification

In order to verify the accuracy of numerical calculation, the experimental pump with guide vane wrap angle of 90° is selected as the prototype model to test the performance curve. As shown in Fig. 3 the numerical simulation results are compared with the experimental values. The results show that the numerical simulation values are in acceptable agreement

with the experimental values, the head and efficiency of the numerical calculation are almost higher than experimental values under various working conditions. This is mainly due to the following two factors: One is that the volume losses caused by leakage of seal and disk friction losses are not taken into account in numerical calculation; the other is that the measured power by experiment is electric power, ignoring the motor losses. Overall, the errors of predicted efficiency and head are all within 3% of the experimental data, the reliability of the numerical result is verified. Therefore, the numerical simulation method can be used to study and analyse the internal flow field of the pump.

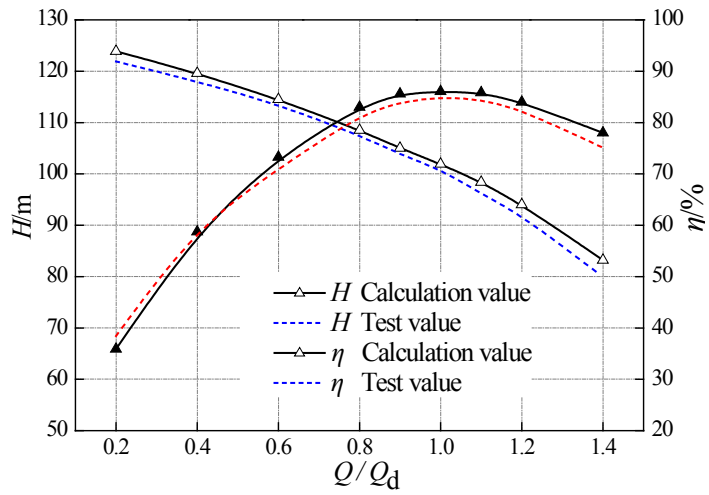

Figure 3: Performance curves of model pump

5 Analysis of results

5.1 Performance analysis

5.1.1 Performance prediction method

After the numerical simulation of the flow field of the pump is completed at design flow rate, the calculation is carried out according to the calculation formula of head and hydraulic efficiency.

The formula for calculating head is as follows:

$$H = \frac{p_{\text{out}} - p_{\text{in}}}{\rho g} \tag{7}$$

The formula for calculating hydraulic efficiency is as follows:

$$\eta = \frac{\rho g H Q}{M \omega} \tag{8}$$

where, P_{out} is the pump outlet total pressure, Pa; P_{in} is the pump inlet total pressure, Pa; ρ is fluid density, kg/m^3; Q is volume flow rate of fluid, m^3/s; M is torque generated by rotation around the shaft, N·s; ω is the rotational angular velocity of the impeller, rad/s.

5.1.2 Performance curves analysis

Under the same setting conditions, the space guide vanes with different wrap angles are assembled with impellers. The relationship between the wrap angle of the space guide vanes and the performance of the submersible pump at design flow rate is obtained by numerical simulation. The calculation results are shown in Fig. 4.

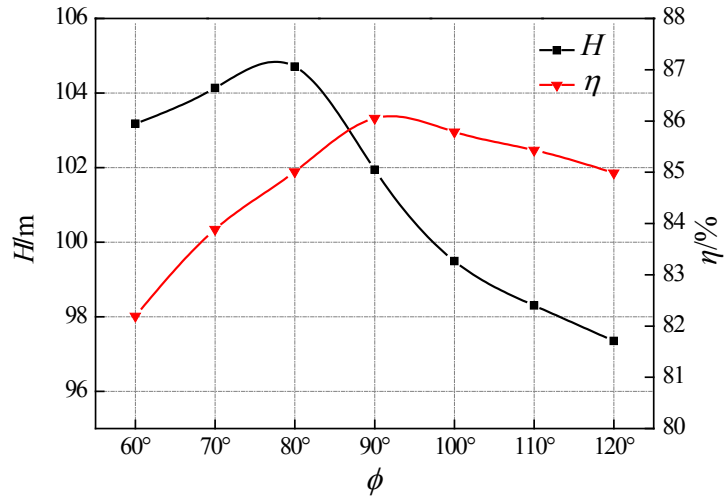

Figure 4: Performance curves of pumps with different guide vane wrap angles

In the relatively smaller wrap angle range, the head and efficiency gradually improve with the wrap angle of the space vane increase. When the wrap angle reaches a certain value, the head and efficiency show a downward trend. It can be noted from the head curve that the head shows upward trend with the wrap angle increase from 60° to 80°, and the head is the maximum when Φ=80°. However, the head declines slightly with the raise of the wrap angle when blade wrap angle is greater than 80°. The efficiency curve presents more obviously upward trend when the wrap angle increases from 60° to 90°. 90° is the best efficiency point, and then the efficiency reduces gradually with the increase of wrap angle.

It can be found that, comprehensive comparison, the head reaches maximum value when Φ=80°, while the efficiency reaches best point when Φ=90°. Within the wrap angle selected in the study, the efficiency increases by about 2.6% approximately, but the increases of head are more significant up to 6.52%. It shows that the change of wrap angle has more obvious effect on head than efficiency, so the guide vane wrap angle should be considered according to the specific performance requirements of submersible pump.

5.2 Hydraulic losses of guide vanes

When the fluid flows into the space guide vane, friction and collision will occur because of the unsmooth wall of the passage and viscosity of the fluid, which will lead to the phenomena of backflow, flow separation and secondary flow of the fluid. All these phenomena will cause hydraulic losses giving rise to head and efficiency decline. Fig. 5 presents the five-stage average relative hydraulic loss of the guide vanes with different wrap angles. The formula for calculating the relative hydraulic loss coefficient λ of guide

vane is defined as the follows:

$$\lambda = \frac{p_1 - p_2}{\Delta p} \times 100\% \tag{9}$$

where, p_1 is the guide vane inlet total pressure, Pa; p_2 is the guide vane outlet total pressure, Pa; Δp is the single stage impeller pressurization value, Pa.

It is found from Fig. 5 that along with the increase of wrap angle, the hydraulic losses of guide vane firstly reduce and then increases, but the hydraulic losses of smaller wrap angle are higher than larger wrap angle. When Φ=80° and Φ=90°, the hydraulic loss is the minimal. It is indicated that the flow separation and collision extent of the fluid in the guide vane is smaller at this wrap angle, so the losses of fluid rotational kinetic energy are smaller. Different wrap angles make the blade shape of the guide vane different. Small wrap angle gives rise to serious fluid diffusion, increases the load on per unit area of the vanes, aggravates hydraulic losses and makes the energy conversion incomplete, so the efficiency is lower. With the increase of the wrap angle, the narrow flow passage of guide vane has more restriction on flow, then, the possibility of deterioration of flow state decelerates, the local head losses decrease, and the efficiency improves. However, the excessive wrap angle makes the flow passage too long, also increases the losses along the walls, and the efficiency declines. Therefore, there is an optimum wrap angle which can make the submersible pump most efficient.

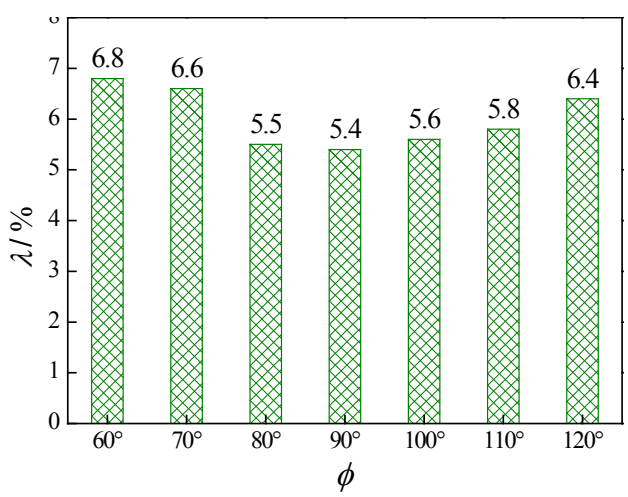

Figure 5: Average hydraulic losses of five-stage guide vanes with different wrap angles

5.3 Turbulent kinetic energy dissipation characteristics

P0~P8, 9 sections perpendicular to the rotation axis of the impeller, are selected to analyse the variation of turbulent kinetic energy dissipation rate ε. As indicated in Fig. 6, P0 and P8 are located in the inlet and outlet of guide vane respectively, and the other sections are evenly distributed along the axis in the guide vane passage.

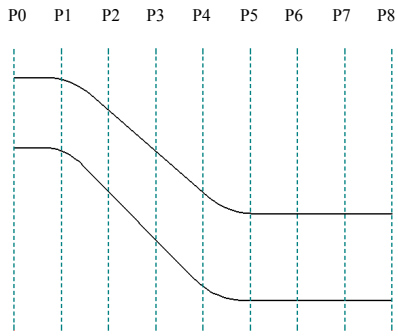

Figure 6: Schematic diagram of the sections

Fig. 7 compares the turbulent kinetic energy dissipation rate in different sections of the guide vane, that is, the conversion rate of fluid mechanical energy dissipates into heat energy in the guide vane. The results show that the variation of turbulent energy dissipation rate along the guide vane passage in different wrap angles is similar. The turbulent kinetic energy dissipation rate at the inlet of the guide vane is higher, and its amplitude tends to be gentle along with the increase of the axial distance. This is mainly due to the high turbulence intensity of the liquid flow from the impeller outlet, and the more vortices generate at the inlet of the guide vane, the greater energy lose. With the liquid flowing into the guide vane, the rectifying effect of the guide vane improves the flow state and reduces the turbulent kinetic energy dissipation rate. Comparing seven curves, with the wrap angle increases from 90° to 120°, the curves change smoothly. And in small wrap angles the turbulent kinetic energy dissipation rate on every section is relatively higher. It indicates that the turbulent kinetic energy at the inlet of the small angle guide vane changes greatly, the fluid diffusivity is higher, and the flow impact loss is serious. With the increase of wrap angle, the turbulent kinetic energy dissipation rate descends and the turbulent in the inlet region is weakened. Therefore, moderate raise of wrap angle can reduce the turbulent losses, improve the energy conversion rate inside of the guide vane, and then the performance of the pump would be enhanced.

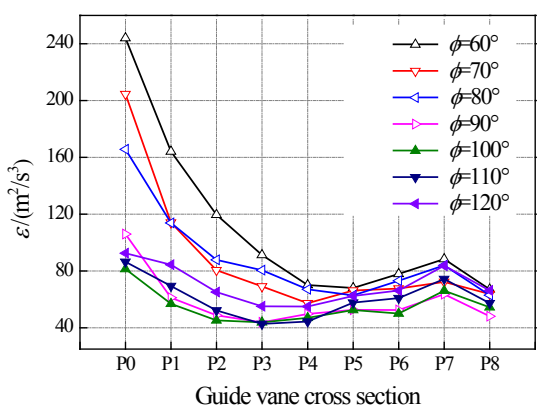

Figure 7: Diagram of the turbulent kinetic energy dissipation on different sections

5.4 Internal flow field characteristics

Four configurations with obvious characteristics which wrap angles are 60°, 80°, 100° and 120° are determined for comparative analysis of the internal flow. Three cross sections P9, P10 and P11 are established to display the flow state, as shown in Fig. 8.

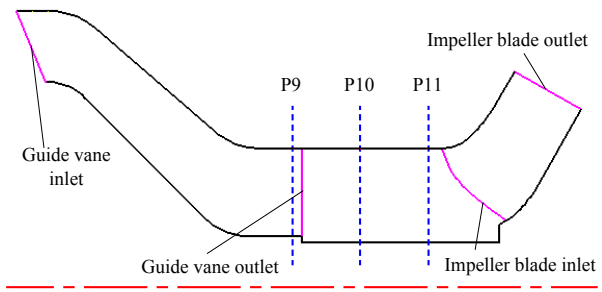

Figure 8: Schematic diagram of sections location

Fig. 9 is velocity contours and velocity streamlines on the selected sections of four wrap angle schemes. As can be seen from the velocity contours, the velocity distribution is different at each wrap angle. When Φ=60°, the low-speed region is relatively larger. The low-speed region reduces when Φ=80°. The distribution of the low-speed region is gradually disordered when Φ=100° and Φ=120°. It is found that there are large or small vortexes on their cross sections. The fact is that the flow through the guide vane still retains a certain residual velocity circulation. Although the rotation movement of this part increases the hydraulic losses of the next impeller, it can maintain a certain rotation into the next stage impeller, and the vortexes hold each other to avoid the expansion of the vortexes. When Φ=60° and Φ=80°, the streamlines distribution on the cross sections presents eight obviously clockwise eddies, which indicates that the shape of the vortexes in the guide vane can be well maintained within smaller wrap angle range. Although the dispersed vortexes increases the energy losses (as shown in the turbulent kinetic energy dissipation characteristics, the turbulent kinetic energy dissipation rate in the guide vane with small wrap angle is higher), when the fluid entrances the next stage impeller, it tends to flow smoothly near the sidewall of the blade and hardly occurs separation phenomenon. A properly rotating fluid can improve properties of the flow and reduce hydraulic losses. Therefore, the average head of the impeller matched with the small angle guide vanes is higher than that of the impeller matched with the large wrap angle guide vanes. When Φ=100° and Φ=120°, the flow lines distribution is extremely disordered, and the dispersed vortexes tend to develop into a large vortex gradually, which weakens the stability at the inlet of the next stage impeller and aggravates the internal losses of the impeller. And the number of small vortexes increases as the enlargement of the wrap angles. Streamlines are distributed in the form of small vortex groups following large ones, so small vortex groups will dissipate the energy transferred by large vortex groups. Therefore, excessive wrap angle worsen the fluid properties at the impeller inlet, which is not conducive to improving the overall performance of submersible well pumps.

In order to study the rectification effect of the guide vanes with different wrap angles in a more clear way, the velocity circulation on the above three cross sections is analysed. As

shown in Fig. 9, R_h and R_r represent the radius of inner ring boundary and outer ring boundary of the guide vane section respectively, and R is the radius of a certain point on the section. The velocity circulation along the radial direction of the guide vane outlet section is shown in Fig. 10. The ξ is the non-dimensional radial position shown as formula (10):

$$\xi = \frac{R - R_h}{R_r - R_h} \tag{10}$$

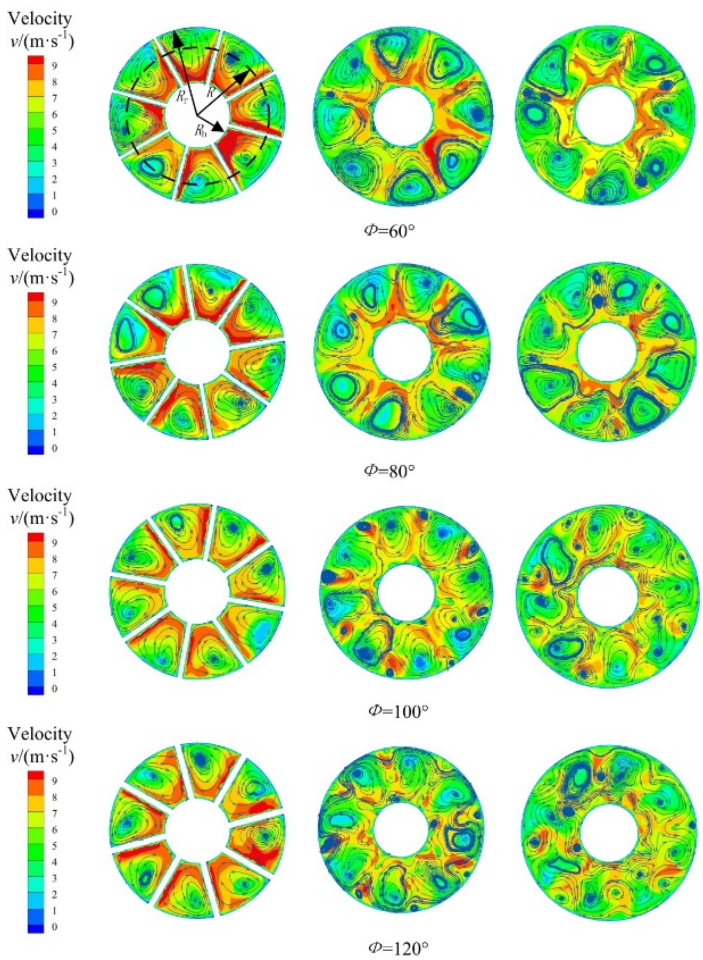

Figure 9: Velocity contours andstreamlines distribution on different sections

From Fig. 10, as can be seen, the variation trend of velocity circulation on P9 section of the four wrap angles is basically the same, and there is negative circulation near the hub region. On P10 section, the circulation curve with the wrap angles of 100° and 120° increases rapidly and the negative circulation area decreases. When Φ=60° and Φ=80°, negative velocity circulation area increases. From the velocity circulation distribution on P11 section, it can be seen that the smaller the wrap angle is, the smoother the curve changes. Generally, different wrap angles change the velocity circulation modes in the bladeless area, but they have little influence on the absolute value of the velocity of the

fluid entering the impeller. In a large area, the velocity circulation on the outlet section of guide vane with smaller wrap angle is close to zero. Therefore, under the schemes of smaller wrap angle, the flow at the impeller inlet is more in line with the non-circulation flow required by the ideal impeller inlet.

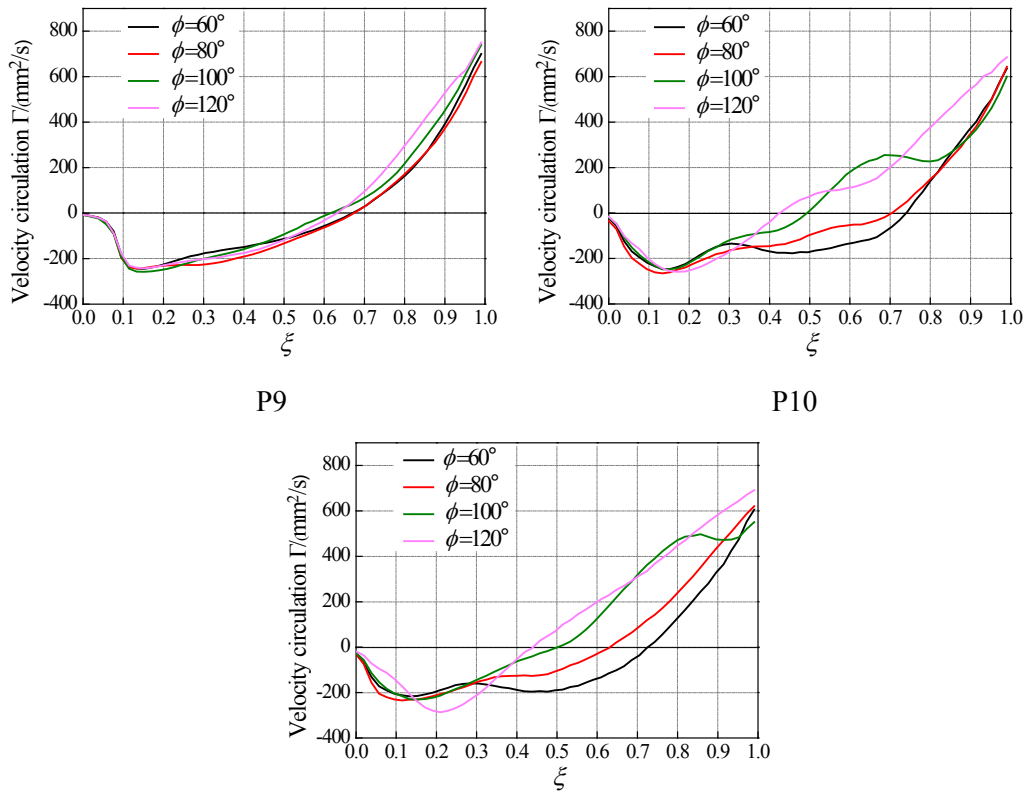

Figure 10: Velocity circulation distribution on the sections of bladeless region

6 Conclusions

1) Through analysing the influence exerted by different wrap angles of the guide vane on the performance of the pump, there are wrap angles that maximizes head and efficiency respectively. In a certain range, the change of the guide vane wrap angle has more significant effect on the head than efficiency. Therefore, the wrap angle of the space guide vane should be considered according to the performance requirements of the pumps.

2) A moderate raise of the wrap angle can enhance properties of the flow, reduce the hydraulic losses and improve the energy conversion ability inside the guide vane.

3) Different wrap angles of the space guide vane affect the distribution modes of the velocity circulation in the bladeless area from guide vane outlet to impeller inlet, and affects the properties of the flow at the inlet of the next stage impeller, but has a weak effect on the absolute value of the velocity circulation of the fluid entering the impeller.

Acknowledgement: This work was supported by the National Natural Science Foundation of China (No. 51469013).

References

Cheng, X. R.; Lv, B. R.; Zhang, X. L.; Wei, Y. Q.; Zhang, S. Y. et al. (2018): Influence of outlet edge position of guide vane on performance of well submersible pump. *Transactions of the Chinese Society of Agricultural Engineering*, vol. 337, no. 10, pp. 76-83.

Chitrakar, S.; Thapa, B. S.; Dahlhaug, O. G.; Neopane, H. P. (2017): Numerical and experimental study of the leakage flow in guide vanes with different hydrofoils. *Journal of Computational Design and Engineering*, vol. 4, no. 3, pp. 218-230.

Cong, X. Q.; Zhou, R.; Han, Y. T.; Yuan, D. Q. (2015): Optimization design of deep-well centrifugal pump based on CFX orthogonal test. *Fluid Machinery*, vol. 43, no. 9, pp. 22-25.

Cresswell, N. W.; Ingram, G. L.; Dominy, R. G. (2015): The impact of diffuser augmentation on a tidal stream turbine. *Ocean Engineering*, vol. 108, no. 12, pp. 155-163.

Guan, X. F. (2011): *Modern Pumps Theory and Design*. China Aerospace Publishing House, China.

Han, W.; Chen, Y.; Liu, Y.; Li, G. X.; Wang, J. et al. (2018): Numerical simulation of end surface erosion characteristicsof hydro-turbine guide vane. *Journal of Drainage and Irrigation Machinery Engineeing*, vol. 36, no. 5, pp. 404-412.

Koirala, R.; Neopane, H. P.; Shrestha, O.; Zhu, B. S.; Thapa, B. (2017): Selection of guide vane profile for erosion handling in Francis turbines. *Renewable Energy*, vol. 112, pp. 328-336.

Liang, J. D.; Lu, L. G.; Xu, L.; Chen, W.; Wang G. (2012): Influence of flow velocity circulation at guide vane outlet of axial-flow pump onhydraulic loss in outlet conduit. *Transactions of the Chinese Society of Agricultural Engineering*, vol. 28, no. 1, pp. 55-60.

Liu, H. L.; Wang, Y.; Liu, D. X.; Yuan, S. Q.; Wang, J. (2013): Assessment of a turbulence model for numerical predictions of sheet-cavitating flows in centrifugal pumps. *Journal of Mechanical Science and Technology*, vol. 9, no. 27, pp. 2743-2750.

Yang, C. X.; Wang, L. (2018): Effect of velocity circulation of flow at guide vane outlet on performance of reactor coolant pump. *Journal of Lanzhou University of Technology*, vol. 44, no. 5, pp. 63-69.

Yang, M. G.; Li, H.; Gao, B.; Liu, D.; Gu, H. F. (2008): Numerical calculation of turbulent flow in a centrifugal pump and flow field analysis to vaned Diffuser. *Fluid Machinery*, vol. 36, no. 7, pp. 16-19.

Zhang, R. H.; Guo, R.; Yang, J. H.; Li, R. N. (2015): Analysis of flow in vane diffuser and its optimization based on CFD method. *Journal of Drainage and Irrigation Machinery Engineering*, vol. 33, no. 9, pp. 762-767.

Zhou, L.; Bai, L.; Yang, Y.; Shi, W. D.; Lu, W. G. (2016): Influence of diffuser vane number on submersible well pump performance. *Transactions of the Chinese Society for Agricultural Machinery*, vol. 47, no. 10, pp. 78-84.

Zhou, L.; Shi, W. D.; Lu, W. G. (2011): Performance analysis on deep-well centrifugal pump guide vanes based on numerical simulation. *Transactions of the Chinese Society of*

Agricultural Engineering, vol. 27, no. 9, pp. 38-42.

Zhou, L.; Shi, W. D.; Lu, W. G.; Xu, R. J.; Wang, C. (2011): Orthogonal test and optimization design of submersiblepump guide vanes. *Journal of Drainage and Irrigation Machinery Engineering*, vol. 29, no. 4, pp. 312-315.

Zhou, S. P.; Hu, L. B.; Zhang, H. (2015): Performance optimization for intermedia stage guide vanes of multistage centrifugal pump. *Transactions of the Chinese Society for Agricultural Machinery*, vol. 46, no. 4, pp. 33-39.